RSC Advances

ROYAL SOCIETY OF CHEMISTRY

www.rsc.org/advances

Journal Name

RSCPublishing

ARTICLE

Fabrication of Triiodothyronine incorporated nanofibrous biomaterial: Its implications on wound healing

Cite this: DOI: 10.1039/xoxxoooooox

Received ooth January 2015,
Accepted ooth January 2015

DOI: 10.1039/xoxxoooooox

www.rsc.org/

Aishwarya Satish,[a] and Purna Sai Korrapati,[a]*

Abstract

With rising incidents of non-healing chronic wounds, functional restoration of the organs after a major wound insult is an essential requisite. The delivery of endogenous molecules through nanomaterials for supporting healing of such wounds has gained impetus in the past decade. Triiodothyronine (T_3) is a hormone that exerts its activity at various target organs and is reported to play a critical role in repair and regeneration of tissues after injury. The encapsulation of T_3 in nanofibers and its sustained release to enable wound healing has been attempted for the first time in this work. The physico-chemical characterization confirmed the encapsulation and uniform distribution of the hormone in the nanofiber. Functional characterization of the composite nanofibers revealed the significant positive influence of the T_3-entrapped nanofibers on the proliferation and migration of skin cells. Thus this work reveals the effect of prolonged sustained delivery of T_3 from nanofibers which might promote the healing of chronic wounds.

Keywords: Triiodothyronine; Sustained release; Cell migration; Wound healing; Nanofibers

Introduction

Wound healing is a major challenge and a topic of interest in research aiming to provide better treatment options to heal chronic non-healing wounds. Hormones are a class of endogenous signaling molecules secreted *in vivo* targeting different organs to regulate physiology and behaviour. Triiodothyronine (T_3), an amino acid derived hormone, is the biologically active lipophilic thyroid hormone[1]. The predominant thyroid prohormone tetraiodothyronine (T_4) is enzymatically cleaved by deiodinases to remove an iodine molecule converting it to the biologically active form[2]. T_3 is one of the most potent stimulators of growth, metabolic rate with a potential role for wound healing and also enhances recovery from stress[3]. Its anabolic and reparative activity has been reported in the tissues and organs like skin, liver, kidney, nervous system, pancreas, lungs, amongst others [4]. The normal serum level of T_3 is approximately 1.5-3.1 nmol/L[5]. T_3 plays an important role in the skin and has the potential to treat several conditions, including disorders of keratinization, alopecia, wound healing and xerosis[3]. It has shown a promising effect on scar-free wound healing and wound contraction[4, 6-9]and its topical delivery through liposome exhibited dose-dependent increase in epidermal proliferation, dermal thickening, and hair growth[10]. Topical treatment with T_3 on mice increased the expression of hair follicular keratinocyte protein (keratin-6), associated with wound healing[7]. It was also shown to heal deep dermal burns by improving the organization of collagen bundles and smoothen the scars[11]. Delivery of T_3 through a biomaterial has previously been explored by encapsulation in PCL nanoparticles as an effective therapeutic for ischemic brain stroke[12].

Intravenous and intraperitoneal delivery of T_3 causes thyrotoxicity due to the excess levels in the systemic circulation leading to catabolic effects like epidermal thinning and inhibition of keratinocytes by the anti-proliferating factors released by fibroblast. Whereas on topical administration, serum T_3 levels were not significantly altered[7, 13] and exhibits direct action on the epidermal cells which in turn encourages wound healing.Azarbayjani et al. developed a polymeric nanofiber system for the topical delivery of thyroxine (T_4) to reduce the deposits of adipose tissue on skin[14]. The group

Biomaterials Department, CSIR-Central Leather Research Institute, Chennai,India-600 020. E-mail: purnasaik.clri@gmail.com; Tel: +91-44-24437263/+91-44-24453491

confirmed the accumulation of biomolecule on the skin surface, minimizing the adverse side effects caused by systemic absorption, using permeation studies in skin model. It was earlier reported that T_3 potentiates insulin signaling and synthesis, illustrating its anti-diabetic role, which could be exploited for healing of diabetic ulcers too[15]. Thus bionanomaterials that encapsulate the hormone, maintain its activity and release it in a suitable manner would be a preferred mode of delivery.

Nanofibers has been chosen as the mode of delivery system as it has a high surface area, good porosity, mechanical properties, nanometer size range[16, 17] and most importantly it mimics the extracellular matrix structure thereby supporting cell attachment and proliferation[18, 19]. The biomolecule can be easily encapsulated in nanofibers by electrospinning the polymer - biomolecule blend without causing loss of the biomolecule as compared to nanoparticle, nanosphere mode of delivery[20]. Polycaprolactone (PCL) is a biodegradable polymer belonging to the aliphatic polyester family. It has been widely used in tissue engineering and wound dressing applications owing to its good mechanical properties, low immunogenicity, slow biodegradability, low toxicity, bioresorbability and high biocompatibility[20-23]. It has also been used as a scaffold for the growth of diverse cell types[22] and as a support polymer it retains the stability of the incorporated biomolecule[17]. On account of its properties, PCL serves as a good drug delivery scaffold.

In this study, T_3, an endogenous biomolecule which is cost effective, has been entrapped in a PCL based nanofiber scaffold system to initiate a sustained release, enabling accelerated wound healing and eliminating systemic seepage of the T_3 hormone.

Results and discussion

Nanofibers and Characterization

T_3 hormone was mixed with polymer solution for electrospinning the hormone encapsulated nanofibers. Polymer concentration and electrical conductivity are important factors that influence the fiber morphology and distribution in electrospinning. 15% PCL was identified as the optimum concentration for electrospinning as the lower concentrations (10% and 12%) resulted in fibers with bead formation (Image not shown here). The voltage of 16 kV and flow rate of 0.4 ml/h were optimized for electrospinning the PCL control and the composite nanofibers. The hormone T_3 was incorporated into PCL nanofibers at increasing concentrations of 0.25, 0.5 and 1 mg/ml of polymer solution, maintaining the same electrospinning parameters. The nanofibers obtained from the combination of 0.25, 0.5 and 1 mg of T_3 per ml of polymer solution are from hereon denoted throughout the work as P/T0.25, P/T0.5 and P/T1 respectively.

The nanofibers were characterized for their morphology, functional groups and thermal properties. Nanofiber samples topographically analyzed by SEM show randomly oriented, continuous fibrous structures in a nanoscale range with interconnected pores (Fig. 1). The diameter for the control PCL electrospun fibers was 200±60 nm. The nanofibers exhibited consistent morphology even with increasing concentration of T_3; however, the composite nanofibers were interspersed with fibers with a broader diameter distribution of 300±100 nm upon hormone loading. This phenomenon has been discussed earlier and broader diameter was reported to favour the proliferation of skin cells [24].

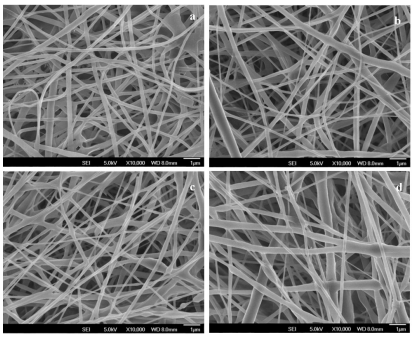

Fig. 1: Scanning Electron Micrographs of a) PCL; b) P/T0.25; c) P/T0.5 and d) P/T1 nanofibers

The encapsulation and distribution of the hormone inside the electrospun PCL nanofibers was confirmed by incorporating FITC labeled T_3 (Fig. 2). The fluorescence image shows the uniform distribution of the hormone entrapped in the nanofiber.

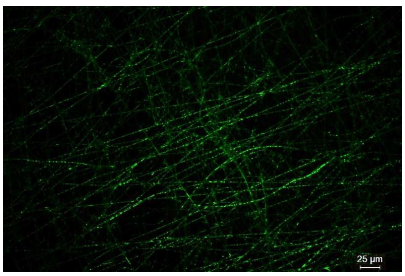

Fig. 2: Fluorescence image of FITC labeled hormone in PCL nanofibers

The PCL-related stretching modes for both the pure polymeric and composite scaffolds were observed in the Infra-Red (FTIR) spectra (Fig. 3). The peaks at 2947 $cm^{-1}$is due to asymmetric CH_2 stretching, symmetric CH_2 stretching at 2866 cm^{-1}, intense sharp peak at 1724 $cm^{-1}$to the carbonyl C=O stretching, C–O and C–C stretching in the crystalline phase at 1293 cm^{-1}, CH_2 bending vibrations at 1465, 1407, and 1362 cm^{-1} and asymmetric COC stretching at 1240 cm^{-1}. The infrared spectrum of T_3 shows peaks concentrated in the region between 1300-1600 cm^{-1} which could be attributed to the aromatic ring and the amine group stretching of the functional groups in T_3 molecule. The IR spectra of the composite nanofibers do not differ from the spectrum of PCL control nanofibers which could be due to the encapsulation of T_3 within the fibers.

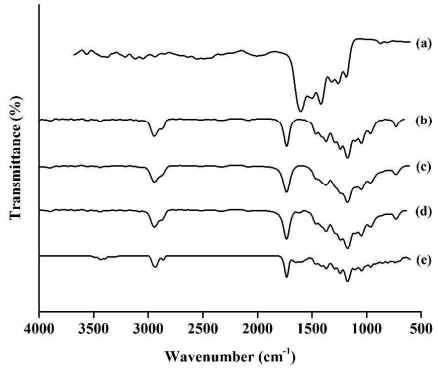

Fig. 3: FTIR spectra of (a) T_3;(b) PCL; (c) P/T0.25; (d) P/T0.5 and (e) P/T1 nanofibers

The melting temperature characteristic of PCL was obtained at 62˚C [25] observed in the DSC thermogram (Fig. 4) The thermogram of the composite nanofibers resemble that of the control polymer. However the endothermic peak observed for P/T0.5 and P/T1 is comparatively broader than that of the control nanofibers and begins at a slightly lower temperature of 60˚C. This minute shift in the peak could be attributed to the entrapment of hormone in the nanofibers and its existence in an amorphous state indicating a thermodynamic compatibility.

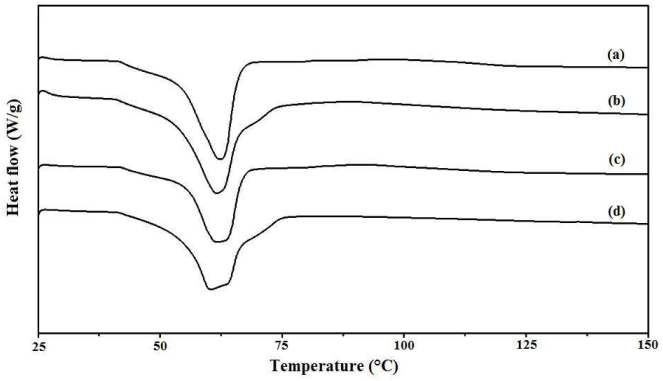

Fig. 4: DSC thermogram of (a) PCL; (b) P/T0.25; (c) P/T0.5 and (d) P/T1 nanofibers

Release profile of T_3 from the fiber (by ELISA method)
The release profile of the hormone from nanofibers is a crucial one. If the level of the hormone exceeds a threshold value *in vivo*, it can turn thyrotoxic. The release of T_3 from PCL nanofibers was determined *in vitro* using ELISA technique considering P/T1 nanofibers as the reference nanofibers and all the results discussed are in terms of ng of T_3 released per mg of the composite nanofiber taken for release (Fig. 5).

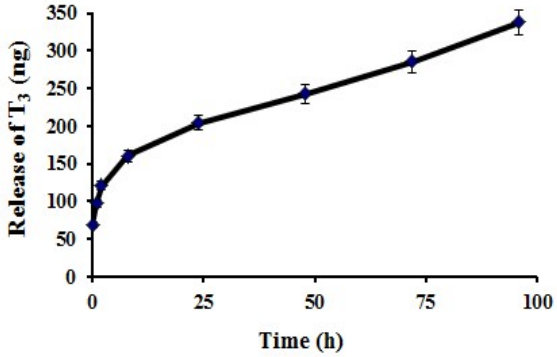

Fig. 5: *In vitro* release profile of T_3 from P/T1 nanofiber in PBS at 37˚C for a period of 4 days. Data is the mean ± SD of three measurements

The initial burst release was curbed to around 70 ng of T_3 after which the release was in a sustained manner. A slow gradual linear release pattern was observed with 200 ng of T_3 on day 1 and 242 ng of T_3 on 2nd day, 286 ng of T_3 on the third day and reaching 340 ng on the fourth day. The release pattern was observed to be in a 40-50 ng increment for every 24 h. The good interaction of hydrophobic polymer (PCL) with the lipophilic drug (T_3) could lead to efficient entrapment and ensure sustained release of the biomolecule from the nanofibers[21]. The nanofiber system of delivery prevents an excess of T_3 to be released, thereby preventing thyrotoxicity and reducing the systemic absorption in the microenvironment. The serum level of T_3 in the range 200 ng/dL - 1,000 ng/dL is thyrotoxic, but is tolerable for a short period by human as reported earlier[10]. In the release profile, it can be noted that on day 4 only 340 ng is released from the nanofiber. Thus this level would be well tolerated when given as a topical therapeutic for wounds and the thyroid hormone status *in vivo* can be maintained when delivered through this nanofiber delivery system.

Proliferation of skin cells in the presence of T_3: MTT assay
Proliferation and migration of cells in the wound border contributes to re-epithelialization and wound contraction.The influence of T_3 released from the nanofibers on the proliferation potential of keratinocytes and fibroblasts were studied by MTT assay and the results are illustrated (Fig. 6). There was an increase in the colour intensity of the purple formazan crystal formation in the composite nanofibers-treated skin cells, which indicated the positive influence of T_3 on the proliferation of cells at day 1 and day 2 time point release.

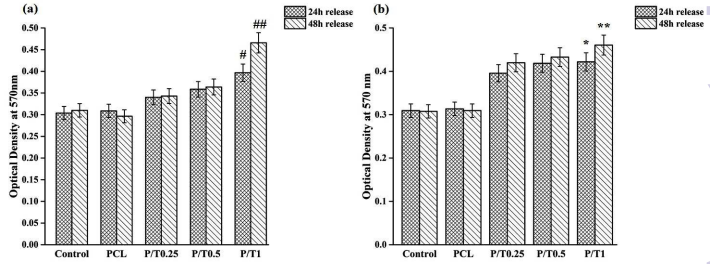

Fig. 6: Effect of the release media collected from composite nanofibers on the proliferation potential of (a) keratinocytes, (b) fibroblasts. The values represent the mean of three repeated experiments with triplicates for each concentration. P-value ($^{\#}$0.031, $^{\#\#}$0.013, *0.027, ** 0.014) was calculated by student's t-test for the indicated concentration by comparing with the untreated cells at the same time point.

Apart from this, the biocompatibility of PCL and its T_3 composite nanofibers directly with the epidermal and dermal cells were tested by MTT assay. The T_3 incorporated nanofibers not only demonstrated excellent compatibility, but also enhanced the proliferation of cells, same as observed with the release media (The results are not displayed here).

The proliferation of both keratinocytes and fibroblasts were accelerated in the composite nanofiber release media when compared to the untreated and PCL treated samples. It was earlier reported that T_3 promotes proliferation of skin cells[9, 10, 13], which suggests that in this study T_3 remains intact even after electrospinning. The cell viability was significantly higher in the 48h release sample of the P/T1 sample, denoting the effectiveness of a higher concentration of T_3 on the proliferation of skin cells. The dose-dependent effect of T_3 on wound healing by the increased epidermal proliferation, dermal thickening and hair growth has been reported earlier[8, 10]. In accordance, this study witnessed a dose-dependent increase in

the proliferation of keratinocytes and fibroblasts with increasing concentration of T_3 entrapped in the nanofiber.

Migration of keratinocytes and fibroblasts in wound margin: *in vitro*scratch wound assay

Re-epithelialization is an important part of wound healing and is facilitated by the migration of skin cells from the wound margins towards the centre of the wound. The effect of T_3 on the promotion of skin cell migration was determined by the enhanced rate of wound closure in a scratch wound model (Fig.7 and Fig.8). The scratch wound was monitored up to 8h time point and the wound area was measured using Image J software[26].

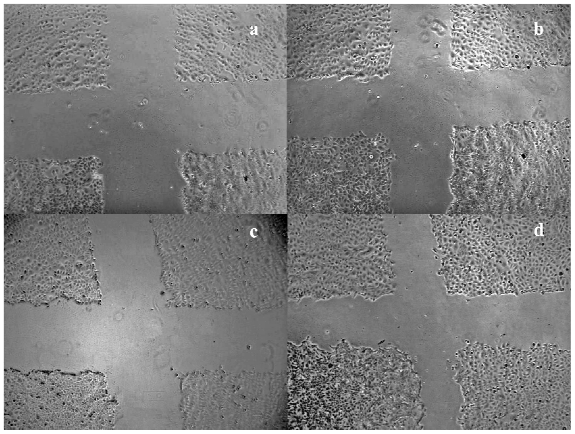

Fig. 7: Representative microscopic images showing the HaCaT migratory pattern in (a & b) untreated and (c & d) T_3-treated cells at (a & c) 0 h and (b & d) 8 h. Scale bar: 100 µm

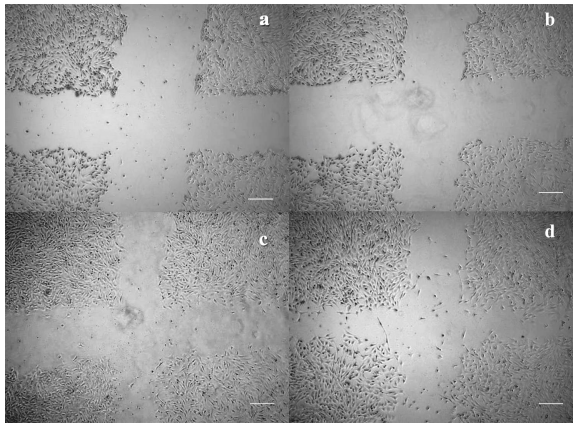

Fig. 8: Representative microscopic images showing NIH 3T3 migratory pattern in (a & b) untreated and (c & d) T_3-treated cells at (a & c) 0 h and (b & d) 8 h. Scale bar: 100 µm

At the 8h time point of day 1 release, percentage of wound recovered was 14 % in the untreated keratinocytes and 23 % in the P/T1 composite nanofibers treated keratinocytes, showing a 9% higher wound closure rate than the control. The percentage of wound recovered at the 8h time point was 23 % in untreated fibroblasts and 43 % in day 1 release of P/T1 composite nanofiber treated fibroblasts, showing nearly double the rate of migration compared to control. Zhang, 2013 had reported that T_4 promoted keratinocytes migration using cortactin, a marker specific for migrating keratinocytes[27]. Thus the actin polymerization, critical to cell migration, could be promoted by T_3 also. Based on the present assay, it was observed that T_3 accelerated migration in a dose-dependent fashion, as the P/T1 scaffold showed the highest keratinocyte and fibroblast migration (Fig. 9).

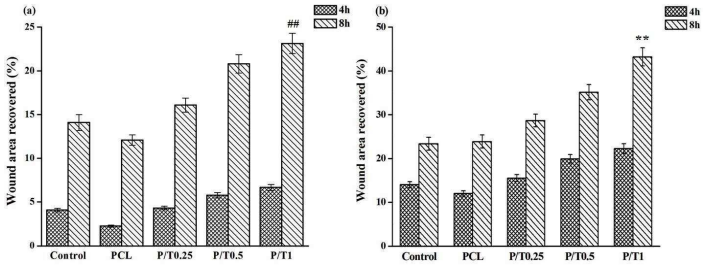

Fig. 9: Graphical depiction of the effect of the day 1 release media on the wound area recovered by migration of (a) keratinocytes, (b) fibroblasts at 4h and 8h time point. *P*-value $^{\#\#}$ 0.033, ** 0.034 were calculated by student's t-test for the indicated concentration by comparing with the untreated cells at the same time point.

As the release media collected from P/T1 nanofibers influenced migration to a higher degree compared to the others, we increased the number of days the release media was collected from P/T1 nanofibers, to examine its effect on wound closure. Thus the release media from P/T1 nanofibers was collected for four consequent days and migration was monitored in the scratch wound model. The results are illustrated in Fig. 10, which represent the percentage of wound closure at 8h time point.

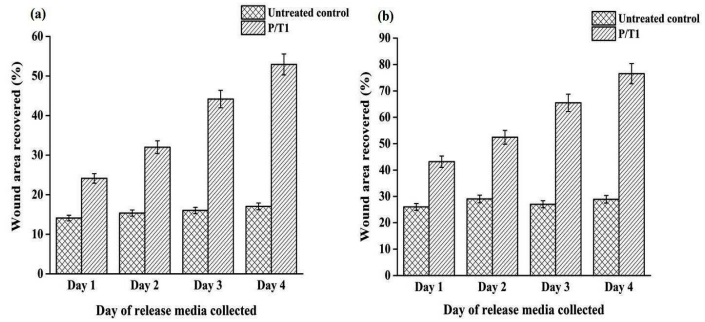

Fig. 10: Effect of extended release media collected from P/T1 nanofiber on the migration of a) HaCaT, b) NIH 3T3 in the 8h time point of the scratch assay.

From the graph (Fig. 10) it is clear that the cells treated with the release media collected from P/T1 nanofibers showed higher percentage of wound closure. In HaCaT cells, 15% of wound area was recovered in the untreated cells compared to 53% in fourth day P/T1 release media (nearly 40% higher than the untreated control). Similarly in NIH 3T3 cells, a 28% wound closure rate was observed in untreated cells compared to 75% in fourth day P/T1 release media (approximately 45% higher). The enhancement in the migration rate of cells in an *in vitro* scratch wound model reflected that the activity of T_3 was retained even on the fourth day of release media collected from the P/T1 composite nanofibers. This could confirm the intact nature of the hormone entrapped in the nanofibers. Based on this study we speculate that this dressing needs to be changed only once in 4 days and is thus advantageous as a wound dressing material.

Migration of mitomycin C pre-treated keratinocytes and fibroblasts: *in vitro*scratch wound assay

The keratinocytes and fibroblasts were treated with mitomycin C, a potent DNA crosslinker to inhibit cell proliferation and confirm that the observed wound area recovery was not due to the T_3 induced proliferation of cells alone (Fig. 11). It could be observed that at 8h and 24h the migration of cells was higher than the untreated control. In the 24h time point, there is a 7% difference in wound closure rate between untreated control (73%) and P/T1 (80%) at day1 release media. At the day 4 time point, there is a 12% increase in wound closure rate of P/T1 (96%) compared to the untreated control (74%). The results suggest that in spite of cell growth arrest, a significant migration in treated cells was observed revealing that T_3 induced migration capabilities and proliferation abilities are independent. Nonetheless the high percentage of wound area recovery observed in the scratch wound assay in the previous section was not observed with mitomycin C treatment of cells discussed in this section, which further confirms the role of T_3 in both cell proliferation and cell migration of skin cells.

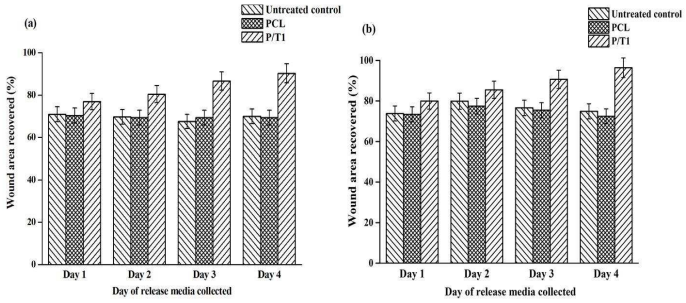

Fig. 11: T_3 induced migration is proliferation independent – (a) keratinocytes and (b) fibroblasts pre-treated with mitomycin C for 2h followed by migration analysis by scratch assay. The values represent the wound closure at 24h post the scratch wound created.

***In vivo* rat wound model and wound closure analysis**

In vivo full thickness excision wounds were created on Wistar rats to monitor the effectiveness of composite T_3 scaffold on wound healing. The wound region was photographed periodically (Fig. 12 (a)). There was no significant difference between the saline and PCL nanofibers treated groups at any time point. The wound area was measured for the control rats (saline, PCL rats) and T_3 treated rats. On day 16, the wound area of control rats had diminished to 14% and 13% (saline, PCL rats) while the wounds in T_3 treated rats displayed nearly complete wound healing. The T_3 treated wounds clearly exhibited a significant acceleration in wound healing when compared to control. In addition it was observed that the rats treated with T_3 had better hair growth compared to control rats. This confirmed the potential of T_3 to promote hair growth [10].

T_3 levels in the blood samples collected from control rats at study entry were 98±8 ng/dL and after 16 days the levels were 110±16 ng/dL. The T_3 levels in the control rats were thus maintained stably over the course of the experiment. In the T_3-treated rats, the levels raised from 116±14 ng/dL to 200±24 ng/dL after 16 days. The increase in the systemic levels of T_3 was much lower than those reported by Safer et al. 2001 in which a liposome based carrier system was used to apply T_3 topically on mice skin[10]. The levels were well within the serum T_3 range 200 ng/dL - 1,000 ng/dL reported to be tolerable. From this it could be inferred that the nanofiber scaffold released T_3 in a sustained manner thereby reducing the amount of T_3 that is seeping into the systemic circulation.

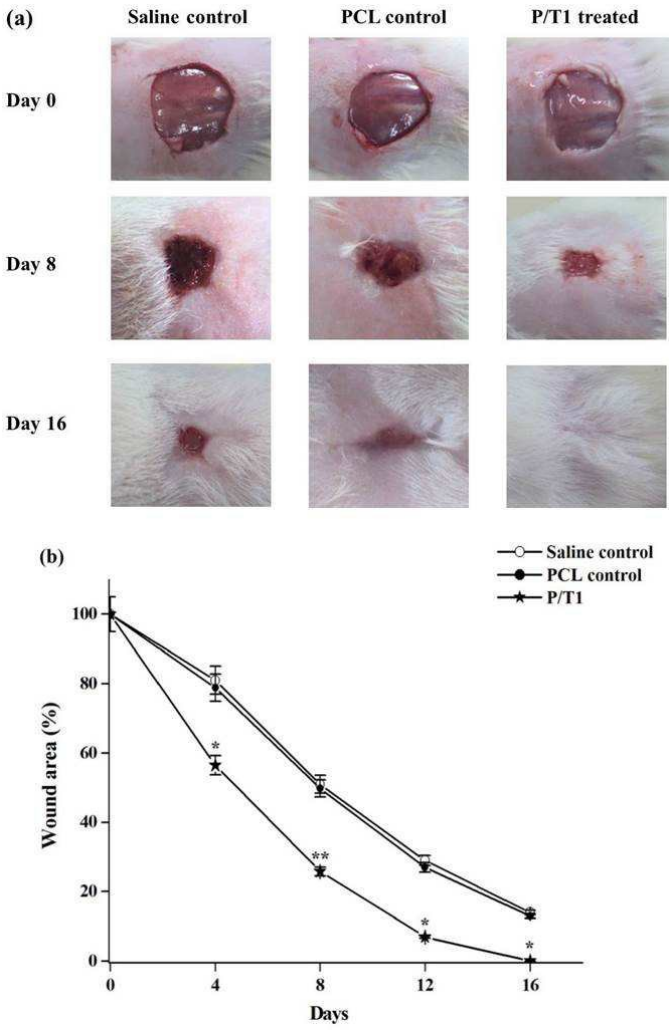

Fig 12: (a) Representative photographs of full thickness excisional wounds treated with saline, PCL nanofibers and P/T1 nanofibers taken on day 0, 8 and 16; (b) Graphical representation of wound closure over time, measured as percentage of original initial wound area. $*P \leq 0.02$ and $**P \leq 0.03$ were calculated by student's t-test for the indicated wound area measured for T_3 treated rats by comparing with the control at the same time point.

Experimental

Materials

Chemicals and Reagents

Polycaprolactone (average M_n 45,000), triiodothyronine, mitomycin C, antibiotics and other chemicals in this study were procured from Sigma-Aldrich, USA. Cell culture media (Dulbecco's Modified Eagle Medium - High Glucose) and Fetal Bovine Serum were from Life Technologies, USA; Mouse Triiodothyronine antibody and Goat Anti-Mouse IgG-HRP secondary antibody used for ELISA were purchased from Santa Cruz Biotechnology, USA. All solvents were of analytical

grade and used without further purification. Deionized water was used throughout the study.

Polymer preparation and Electrospinning

Polycaprolactone (PCL) was dissolved at 15% (w/v) in Dichloromethane : Ethanol at a ratio of 1:1 (v/v). T_3 of various concentrations (0.25, 0.5 and 1 mg per ml of polymer solution) were added to the polymer solution and was thoroughly stirred for 2-3 h. The blend solution was loaded in a 2 ml syringe equipped with an 18-gauge blunt stainless steel needle and was electrospun by controlling the feeding rate using a syringe pump (physics instrument & co., India) at 0.4 ml/h. Electric potential of 16 kV was applied to the metallic needle (0.5 mm inner hole diameter) and the tip to collector distance was set at 12-15 cm. On application of electric potential, the jet breaks up into fibers from the Taylor cone and gave rise to relatively dry fibers which were subsequently collected on aluminium foil and cover slips until a thick fiber mat was obtained. The electrospinning process was carried out at 24 ± 1° C and relative humidity of 68 ± 3° C in an enclosed Plexiglas box.

Nanofiber Characterization

The surface morphology and the diameter of the prepared nanofibers were analyzed by scanning electron microscopy (SEM) (Hitachi, Japan) using an acceleration voltage of 10 kV. The samples were gold sputter coated under argon atmosphere to render them electrically conductive prior to SEM. The diameter of the electrospun nanofibers were measured for a minimum of 50 fibers in each of the sample set using Image J software and the average diameter was calculated. To ensure the presence and distribution of the hormone incorporated in the electrospun PCL nanofiber scaffolds, T_3 was conjugated with FITC [28] and stirred with the polymer solution. A thin layer of the electrospun fibers were collected on a glass slide and observed under fluorescence microscope (Leica microsystems, Germany). Functional groups of the composite nanofiber samples were characterized using Fourier Transform Infrared (FTIR) spectrometer (Perkin-Elmer, USA). The samples were cut into small pieces, ground with KBr and pressed into pellets. Measurements were taken in a range between 4000 - 500 cm^{-1} with a resolution of 2 cm^{-1}. The thermal behaviour of the nanofiber samples were determined using differential scanning calorimeter (DSC) apparatus (Q200 V23.10, TA Instruments, USA). Samples were hermetically sealed in standard aluminium pans and heated at a constant rate of 10°C min^{-1}. The thermograms of the samples were recorded from 25°C to 150°C in an inert nitrogen atmosphere.

Release profile of T_3 from the fiber (ELISA method)

The release of T_3 from the electrospun nanofibers (P/T1 nanofibers was taken as the representative composite nanofiber and compared to control PCL nanofibers) was quantitated by ELISA. Briefly, approximately 1 mg of nanofiber samples (P/T1 and control nanofibers individually) were weighed separately for each time point such as 0h, 1h, 2h, 8h, 24h, 48h, 72h and 96h in microfuge tubes. To each of these tubes, 1 ml of 0.01M phosphate buffer (pH 7.4) was added and incubated at 37 °C. 500 µl of buffer solution was collected from each sample tube at the denoted time and stored at 2-8° C until the remaining release samples were collected. The collected sample solutions (200 µl) were coated on the ELISA plate and allowed for overnight incubation at 2-8° C. The release pattern of T_3 from nanofibers was determined by ELISA technique using a T_3 antibody and a HRP conjugated secondary antibody following the standard ELISA protocol (Indirect ELISA, Sigma-Aldrich Protocols).

Cell culture

Immortalized human epidermal keratinocytes, HaCaT and mouse NIH 3T3 fibroblasts were obtained from National Centre for Cell Science, Pune, India. The cells were cultured in complete Dulbecco's Modified Eagle Medium with streptomycin (100 µg/ml), penicillin (100 units/ml), gentamicin (30 µg/ml) and amphotericin B (2.5 µg/ml) procured from Life Technologies. The cells were maintained at 37 °C in a humidified 5% CO_2 incubator (Binder, Germany) in 25 cm^2 culture flasks.

Sample release media collection

Nanofiber samples (PCL, P/T0.25, P/T0.5 and P/T1) were taken in triplicates for two time points, at a concentration of 1 mg nanofiber sample per ml of serum-free DMEM medium. Samples were incubated in a sterile 37 °C chamber. A sample containing only serum-free DMEM medium was also incubated under the same conditions and was considered as blank. At day 1 and day 2, the release medium was collected from the respective tubes and used for further assays.

Skin cells proliferation in the presence of T_3: MTT assay

The proliferation of keratinocytes and fibroblasts in presence of the nanofibers and sample release medium was evaluated by MTT (3-(4,5-Dimethylthiazol-2-yl)-2,5-diphenyltetrazolium bromide) assay protocol[29]. For the assay, 12×10^3 HaCaT cells/well and NIH 3T3 cells/well were seeded separately in 48 well tissue culture plates. Following overnight incubation, the sample release media (collected prior to the assay as explained in previous section) were added in triplicates for each sample type. In case of direct treatment with nanofibers, 0.25 mg nanofiber samples of each type was weighed in triplicates, and added to each well of a 48-well tissue culture plate. On addition of media the concentration of the nanofiber sample would be 1 mg/ml of media in each well. Over these fibers, 12×10^3 cells/well were seeded and incubated overnight. After 24 h, the cells were treated with MTT (0.5 mg/ml in PBS) and incubated for 3 hours at 37 °C. DMSO was used to dissolve the formazan complex formed by the live cells and the intensity of the color was measured colorimetrically at 570/630 nm using a micro plate reader (Bio-Rad, USA).

Migration of keratinocytes and fibroblasts in wound margin: *in vitro* scratch wound assay

2×10^5 keratinocytes (HaCaT), and 1.6×10^5 fibroblasts (NIH 3T3) at passage 3 were separately seeded per well in 24 well tissue culture plate in DMEM medium with 10% serum, until confluence in a CO_2 incubator. Thereafter, a scratch wound was created on the monolayer of cells using a 200 µL pipette tip followed by a wash with PBS. The sample release medium collected freshly prior to the assay (as elaborated previously) was added to each well. The migration of cells was captured using a phase contrast microscope (Leica Microsystems, Germany) at a time interval of 4 h and the wound area was measured using Image J software [26]. The percentage of wound recovered was calculated using the formula mentioned below, and the significance was computed using student's t-test.

$$\text{Wound area recovered (\%)} = \frac{\text{(Initial wound area - Final wound area)}}{\text{Initial wound area}} \times 100$$

Migration of Mitomycin C treated keratinocytes and fibroblasts: *in vitro* scratch wound assay

Mitomycin C is a potent DNA crosslinker and halts the proliferation of cells. To ensure that the effect of T_3 on the migration of the skin cells was not dependent on cell proliferation, the cells were pre-treated with 10 µg/ml of mitomycin C for 2 h. The cells were washed thrice with phosphate buffer after which scratch wound was created[30, 31]. The wound area was monitored using phase contrast microscope (Leica Microsystems, Germany) at a time interval of 4 h and measured using Image J software [26]. The percentage of wound recovered was calculated using the formula mentioned below, and the significance was computed using student's t-test.

$$\text{Wound area recovered (\%)} = \frac{\text{(Initial wound area - Final wound area)}}{\text{Initial wound area}} \times 100$$

In vivo rat wound model and wound closure analysis

Female albino Wistar rats (12 in number) weighing ~ 180 g were purchased. The rats were divided into three groups: two control groups 1) saline (4 numbers) and 2) PCL nanofibers (4 numbers) while the experimental group (4 numbers) was treated with 3) P/T1 nanofibers. The pelage of rats was shaved at the dorsal surface below the cervical region. Uniform sized open excision type wounds of 6 cm^2 were created under mild anaesthesia (intraperitoneal injection of ketamine (100mg/kg) and xylazine (10 mg/kg). Wounds were photographed and wound area was measured by tracing the wound margin in a transparent graph sheet. The percentage of wound healing was calculated using the following formula, and the significance was computed using student's t-test.

$$\text{Wound healing (\%)} = \frac{\text{(Initial wound area - Wound area on day } n\text{)}}{\text{Initial wound area}} \times 100$$

This procedure was continued till the wounds were completely healed. Blood samples were collected by retro-orbital bleeding at the start and on the 16^{th} day of study from saline, PCL control and T_3 treated rats. The T_3 levels were determined by ELISA as elaborated previously. All experiments were carried out after obtaining approval from the institutional animal ethical committee.

Statistical analysis

All the experiments and the values represented in the work are the mean of three repeated experiments with triplicates for each concentration.

Conclusions

T_3 entrapped nanofibers were designed such that the biomolecule is released in a sustained manner thereby preventing thyrotoxicity caused by the excess levels due to systemic seepage. The dose-dependent enhancement of both proliferation and migration of keratinocytes and fibroblasts confirms the potential of the T_3 composite nanofibers for wound healing. In addition, the time extended migration analysis for P/T1 nanofibers suggests that the scaffold can be effectively used as wound dressing material for a period of 4 days avoiding frequent replacements. T_3 is comparatively inexpensive and has a potential for treatment of chronic wounds and diabetic ulcers. The study therefore highlights the potential of nanofiber mediated sustained delivery of T_3 to effectively enhance the healing of wounds.

Acknowledgements

The authors are grateful to the Director, CSIR – CLRI for his constant support. The first author would like to acknowledge the DST-INSPIRE programme, New Delhi for the research fellowship (IF130876).

References

1. A. J. Hulbert, *Biological Review*, 2000, **75**, 519-631.
2. J. D. Safer, *Journal of Thyroid Research*, 2013, **2013**, 1-5.
3. J. D. Safer and M. F. Holick, in *Thyroid Disorders with Cutaneous Manifestations*, ed. W. R. Heymann, Springer-Verlag London Limited, 2008, vol. 14, pp. 181-186.
4. I. Mourouzis, E. Politi and C. Pantos, *Journal of Thyroid Research*, 2013, **2013**, 1-5.
5. I. E. Brajkovich, K. Mashiter, G. F. Joplin and J. Cassar, *Metabolism* 1983, **32**, 745-747.
6. D. Antonini, A. Sibilio, M. Dentice and C. Missero, *Frontiers in Endocrinology*, 2013, **4**.
7. J. D. Safer, T. M. Crawford and M. F. Holick, *Endocrinology*, 2005, **146**, 4425-4430.
8. R. Kassem, Z. Liberty, M. Babaev, H. Trau and O. Cohen, *Clinical and Experimental Dermatology*, 2012, **37**, 850-856.
9. M. Tarameshloo, M. Norouzian, S. Zarein-Dolab, M. Dadpay, J. Mohsenifar and R. Gazor, *Anatomy & Cell Biology*, 2012, **45**, 170.
10. J. D. Safer, L. M. Fraser, S. Ray and M. F. Holick, *Thyroid*, 2001, **11**, 717-724.
11. A. H. Mehregan and P. Zamick, *Journal of Cutaneous Pathology*, 1974, **1**, 113-116.
12. A. Mdzinarishvili, V. Sutariya, P. K. Talasila, W. J. Geldenhuys and P. Sadana, *Drug delivery and translational research*, 2013, **3**, 309-317.
13. J. D. Safer, T. M. Crawford, L. M. Fraser, M. Hoa, S. Ray, T. C. Chen, K. Persons and M. F. Holick, *Thyroid*, 2003, **13**, 159- 165.
14. A. F. Azarbayjani, J. R. Venugopal, S. Ramakrishna, P. F. C. Lim, Y. W. Chan and S. Y. Chan, *Journal of Pharmcology and Pharmaceutical Science*, 2010, **13**, 400-410.
15. Y. Lin and Z. Sun, *British Journal of Pharmacology*, 2011, **162** 597–610.
16. E.-R. Kenawy, F. I. Abdel-Hay, M. H. El-Newehy and G. E. Wnek, *Materials Chemistry and Physics*, 2009, **113**, 296-302.
17. K. Madhaiyan, R. Sridhar, S. Sundarrajan, J. R. Venugopal and S. Ramakrishna, *International journal of pharmaceutics*, 2013, **444**, 70-76.
18. C. P. Barnes, S. A. Sell, E. D. Boland, D. G. Simpson and G. L. Bowlin, *Advanced drug delivery reviews*, 2007, **59**, 1413-1433.
19. S. Agarwal, J. H. Wendorff and A. Greiner, *Polymer*, 2008, **49**, 5603-5621.
20. G. A. Montero, J. M. Gluck and M. W. King, Strasbourg, 2005.
21. H. T. Bui, O. H. Chung, J. Dela Cruz and J. S. Park, *Macromolecular Research*, 2014, **22**, 1288-1296.

22. M. Alves da Silva, A. Crawford, J. Mundy, A. Martins, J. V. Araujo, P. V. Hatton, R. L. Reis and N. M. Neves, *Tissue Engineering: Part A*, 2009, **15**, 377-385.
23. P. Karuppuswamy, J. Reddy Venugopal, B. Navaneethan, A. Luwang Laiva and S. Ramakrishna, *Materials Letters*, 2015, **141**, 180-186.
24. J. G. Merrell, S. W. McLaughlin, L. Tie, C. T. Laurencin, A. F. Chen and L. S. Nair, *Clin Exp Pharmacol Physiol*, 2009, **36**, 1149-1156.
25. D. Paneva, F. Bougard, N. Manolova, P. Dubois and I. Rashkov, *European Polymer Journal*, 2008, **44**, 566-578.
26. M. D. Abràmoff, P. J. Magalhães and S. J. Ram, *Biophotonics International*, 2004, **7**, 36–42.
27. G.-Y. Zhang, doctorate, University of Lübeck, 2013.
28. D. Fuquan and C. Yi, *Science China Chemistry*, 1999, **42**, 663-669.
29. T. Mosmann, *Journal of lmmunological Methods*, 1983, **65**, 55-63.
30. Y. Liu, M. Petreaca, M. Yao and M. Martins-Green, *BMC cell biology*, 2009, **10**, 1.
31. I. Haase, R. Evans, R. Pofahl and F. M. Watt, *Journal of Cell Science*, 2003, **116**, 3227-3238.

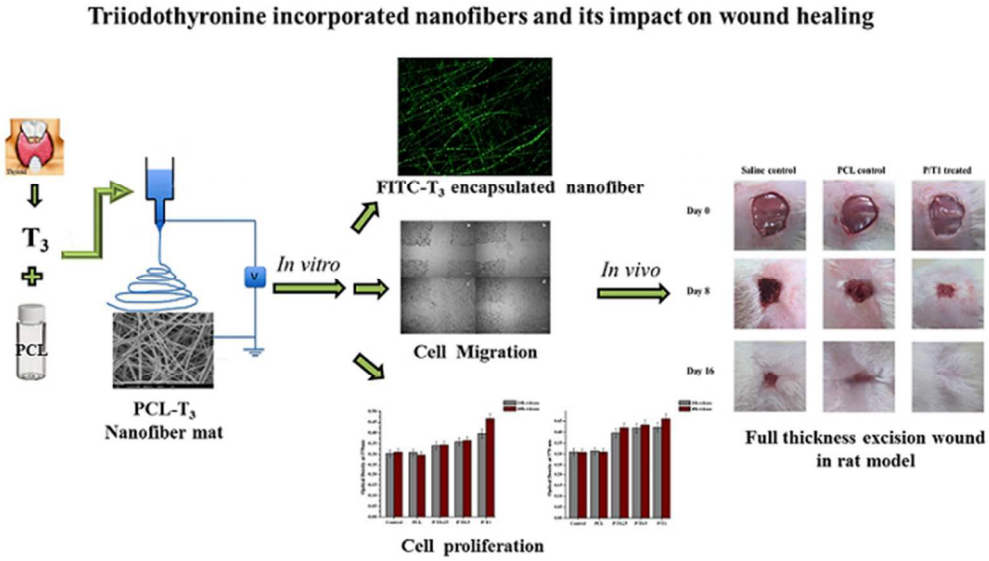

Triiodothyronine incorporated nanofibers and its impact on wound healing

187x107mm (96 x 96 DPI)